

Numerical Simulation of Toner Transfer Considering Voltage Distribution on the Transfer Belt

Shinji Aoki[^], Masaki Sukesako and Masami Kadonaga

Imaging Engine Development Division, Ricoh Company, Ltd., 810 Shimoimaizumi, Ebina-shi,
Kanagawa 243-0460, Japan
E-mail: shinji.st.aoki@nts.ricoh.co.jp

Abstract. A simplified simulation method coupling two-dimensional (2D) and three-dimensional (3D) models is proposed for analysis of primary toner transfer processes. In the 2D model, the electric potential distribution of a vicinity of a transfer nip is simulated including conditions and configurations of the transfer process. Meanwhile, the motion of toner particles is simulated with a 3D parallel plate model, including the relation between the electric potential of the intermediate transfer belt and the transfer gap obtained by the 2D simulation. The validity of the 2D and the 3D models is separately examined, and analyses of a primary transfer process in a printer have been demonstrated using the coupling method. The method has nicely reproduced transfer phenomena with small computational load. © 2008 Society for Imaging Science and Technology. [DOI: 10.2352/J.ImagingSci.Technol.(2008)52:5(051001)]

INTRODUCTION

Intermediate transfer systems have been widely used in electrophotographic printers. In these systems, a toner image developed on a photoconductor is primarily transferred onto an intermediate transfer member and then secondarily transferred onto a sheet of paper. As toner images are transferred by the electrostatic force, design of the electric field distribution in transfer processes is a key point for faithful transfer. Recently numerical methods have been applied to analysis of the electric field.¹⁻⁵

In numerical analysis of transfer processes, a calculation grid dimension smaller than the diameter of toner particles is suitable for prediction of the transferred toner images, as the strength and the direction of the electrostatic force on individual toner particles, which determine the image quality, can be evaluated precisely. On the other hand, if the vicinity of a transfer nip is modeled using such a small size of calculation grids, the number of calculation grids becomes large and considerable computational load is required, especially in three-dimensional (3D) analysis.

In the present work, a simulation method of a transfer process, which can predict transferred images with small computational load, is proposed and analyses of a primary transfer process are demonstrated.

[^]IS&T Member.

Received Dec. 12, 2007; accepted for publication Mar. 17, 2008; published online Sep. 19, 2008.

1062-3701/2008/52(5)/051001/6/\$20.00.

SIMULATION PROCEDURE AND MODEL

In the simulation method, the motion of toner particles between an organic photoconductor (OPC) and an intermediate transfer belt (ITB) is simulated with a 3D parallel plate model, whereas the electric potential of the ITB obtained by a two-dimensional (2D) electric field simulation is applied to a boundary condition. The simulation procedure is shown in Figure 1 and the models of the 2D and the 3D simulation are described in the following.

Two-Dimensional Model

First, the vicinity of a transfer nip in a printer is modeled in a 2D boundary-fitted coordinate system. An example of the 2D model is shown in Figure 2, and a schematic illustration around the transfer nip is shown in Figure 3. Toner is dealt with as a layer, and it is set on the OPC in the prenip region and on the ITB in the postnip region. The thickness and the volume charge density of the toner layer are changed depending on the developed amount of toner, the charge amount of toner, and image area ratio. At the initial state, a uniform electric charge is distributed on the OPC surface,

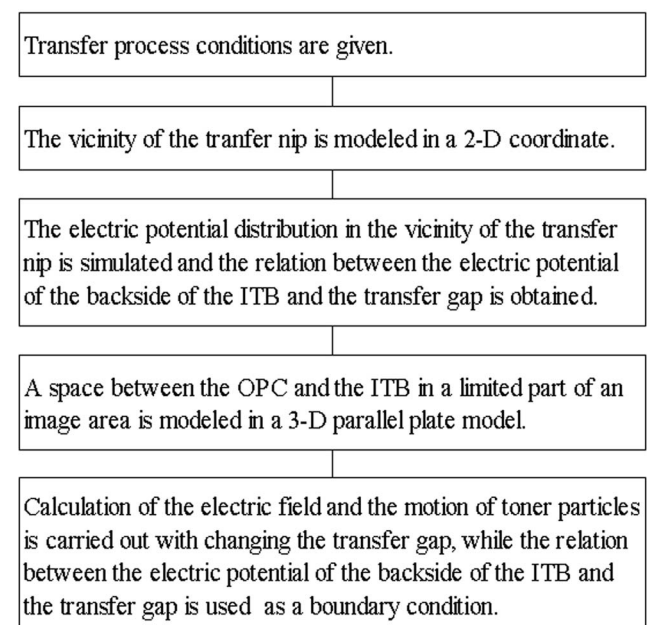


Figure 1. Simulation procedure.

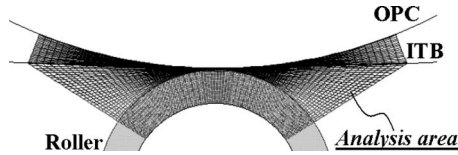


Figure 2. Schematic illustration of the 2D model.

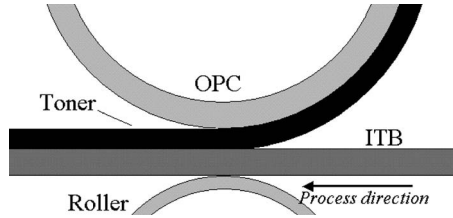


Figure 3. Schematic illustration around the transfer nip in the 2D model.

and the amount is also varied according to the charging potential and image area ratio.

After the arrangement of the OPC, the toner layer, and transfer members, the electric potential distribution is calculated taking into consideration the transfer bias, electrical characteristics of transfer members, the transport of electric charge, and the electrostatic discharge.

The electric field \mathbf{E} and the electric potential ϕ in the analysis area are solved with the Poisson equation:

$$\operatorname{div} \mathbf{E} = -\operatorname{div}(\operatorname{grad} \phi) = \rho/\varepsilon, \quad (1)$$

where ρ is the electric charge density and ε is the permittivity.

The electric charge density ρ is obtained by considering the transport of the electric charge and the discharge. The transport of the electric charge is expressed by the equation of continuity:

$$\partial \rho / \partial t = -\operatorname{div} \mathbf{J}, \quad (2)$$

where t is the time and \mathbf{J} is the current density.

The current density \mathbf{J} is calculated including the electrical conduction and the advection as follows:

$$\mathbf{J} = \sigma \mathbf{E} + \rho \mathbf{v}_p, \quad (3)$$

where σ is the electrical conductivity and \mathbf{v}_p is the process velocity of the printer.

In the case where the ITB is made of such a carbon-filled plastic, the electric field dependence of the electrical conductivity σ is considered. In the present model, the field dependence of the electrical conductivity σ is reflected using the Poole-Frenkel law:⁶

$$\sigma = \alpha \exp(\beta |\mathbf{E}|^{1/2}), \quad (4)$$

where α and β are empirical constants determined by a resistivity measurement.

The effect of discharge is considered by adding electric charge on objects forming an air gap, when the electric po-

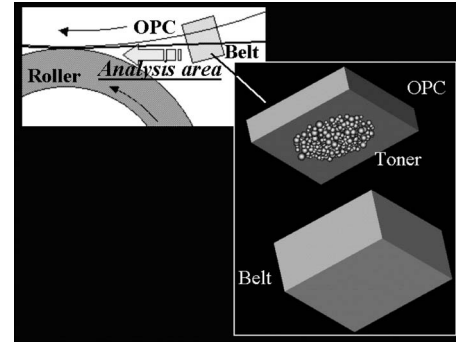


Figure 4. Schematic illustration of the 3D model.

tential difference across the air gap exceeds the Paschen limit. The relations between the Paschen limit ϕ_{pa} , in units of volts, and the air gap G , in units of meters, are as follows:⁷

$$\phi_{pa} = \begin{cases} 75.4 \times 10^6 G & (G < 4.8 \times 10^{-6}) \\ 362 & (8 \times 10^{-6} \geq G \geq 4.8 \times 10^{-6}) \\ 312 + 6.2 \times 10^6 G & (G > 8 \times 10^{-6}). \end{cases} \quad (5)$$

The amount of the discharge Q , in Coulombs per square meter, is estimated by the following equation:

$$Q = \varepsilon_0 (\Delta \phi - \phi_{pa}) \left[\sum (d_i / \varepsilon_i) + G \right] / \left[G \sum (d_i / \varepsilon_i) \right], \quad (6)$$

where $\Delta \phi$ is the electric potential difference across the air gap in units of volts, ε_0 is the vacuum permittivity, and ε_i and d_i are the relative dielectric constant and the thickness of an object, respectively. The previous equations are solved until a steady state ($\partial E / \partial t = 0$) is reached and the relation between the electric potential of the back side of the ITB and the transfer gap is obtained.

Three-Dimensional Model

Second, a space between a part of the toner image on the OPC and the ITB is modeled in a 3D parallel plate model with the calculation grids smaller than the diameter of the toner particles. Then calculation of the electric field and the motion of toner particles is carried out by changing the transfer gap, whereas the relation between the electric potential of the back side of the ITB and the transfer gap obtained by the 2D simulation is used as a boundary condition. At the initial state, the latent image and toner particles exist on the surface of the OPC, and toner particles adhere to the OPC by electrostatic and nonelectrostatic forces. An example of the 3D model is shown in Figure 4.

The electric field \mathbf{E} and the electric potential ϕ are solved again by the Poisson equation [Eq. (1)] with consideration of the Paschen discharge [Eqs. (5) and (6)]. In the present work, the discharge between the OPC and the ITB, toner on the OPC and the ITB, the OPC and toner on the ITB, and toner on the OPC and toner on the ITB is considered.

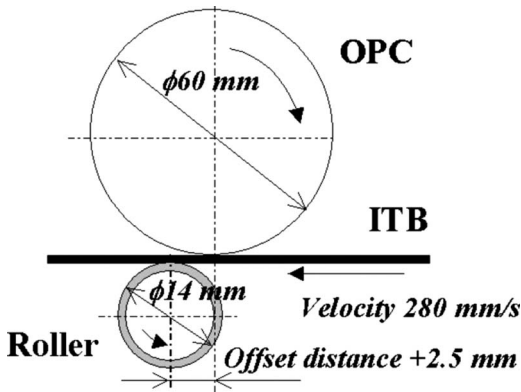


Figure 5. Schematic illustration of the primary transfer process.

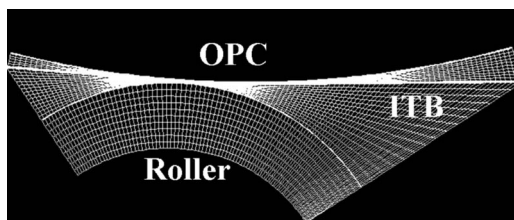


Figure 6. Calculation grid used for the 2D model validation.

The electrostatic force acting on a toner particle F_e is related to the quantity of electric charge of the toner particle q and the electric field E as

$$F_e = qE, \quad (7)$$

and the motion of the toner particle is calculated by Newton's second law of motion:

$$F_e = d(m_t v_t) / dt, \quad (8)$$

where m_t and v_t are the mass and the velocity of the toner particle, respectively.

In the present model, the toner particle begins to move when the electrostatic force acting on the toner particle F_e overcomes the nonelectrostatic adhesion force, and continues to move until it reaches the surface of the ITB. Collisions between toner particles are not considered.

EXPERIMENTAL VALIDATION OF THE SIMULATION MODELS

Before analyzing transfer processes in printers, validation experiments for the 2D and the 3D models were separately carried out as follows.

Validation of the 2D Model

The validity of the 2D model was examined by comparing experimental and calculated results of relationships between the applied voltage and the current of a primary transfer process in a printer. A schematic illustration of the primary transfer process is shown in Figure 5, and the calculation grid used for the simulation is shown in Figure 6. The ITB was made of a carbon black filled polyimide; then the field

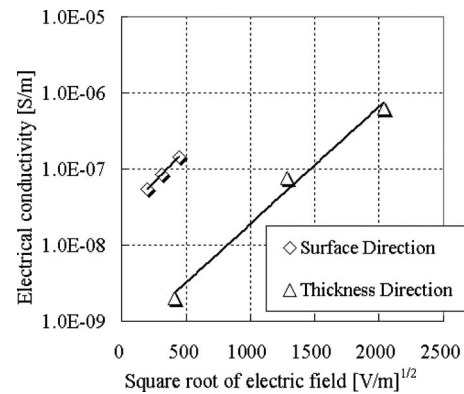


Figure 7. Characteristics of the electrical conductivity of the intermediate transfer belt.

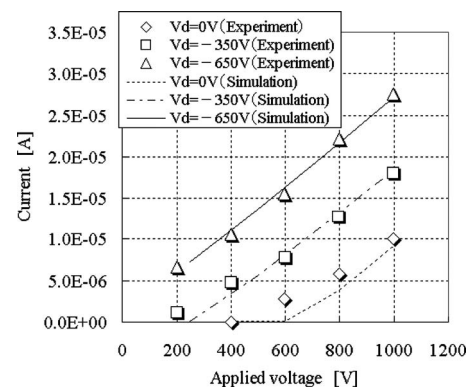


Figure 8. Relationships between the applied voltage and the current of the primary transfer process.

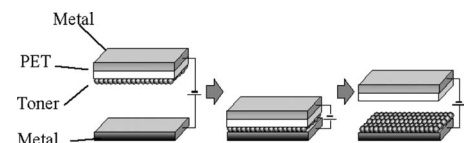


Figure 9. Schematic illustration of the model experiment.

dependence and the anisotropic nature of the electrical conductivity were considered in the calculation. Figure 7 shows the characteristics of the electrical conductivity of the ITB. On the other hand, a constant electrical conductivity ($0.1 \mu\text{S/m}$) was used for the primary transfer roller, as its material shows the Ohmic conduction. The OPC is treated as an insulator.

Shown in Figure 8 are experimental and calculated results with various surface electric potential of the OPC (V_d) on the condition that the toner is not developed. The good agreement indicates that the electric field distribution is properly simulated by this model.

Validation of the 3D Model

The validity of the 3D model was examined with a simple model experiment, where the applied voltage dependence of the transfer efficiency was studied. A schematic illustration of the model experiment is shown in Figure 9. Developed

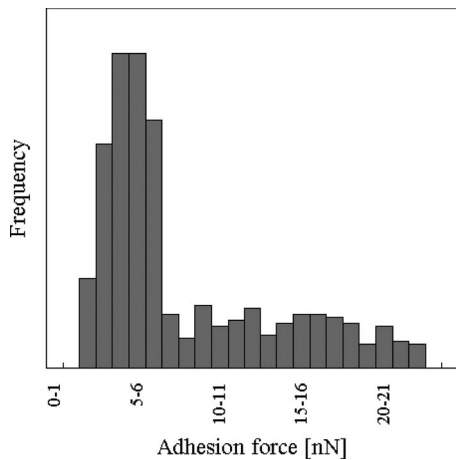


Figure 10. Distribution of the nonelectrostatic adhesion force of toner particles used for the 3D model validation.

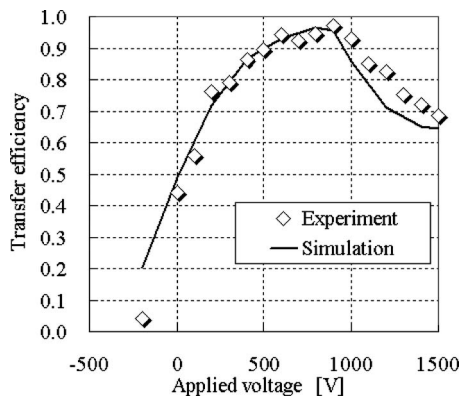


Figure 11. Applied voltage dependence of the transfer efficiency in the model experiment.

toner on a polyethylene terephthalate (PET) coated metal plate was made to approach a facing metal plate until contact was established, and then separated; a constant voltage difference was applied between the metal plates throughout. The amount of developed toner was 1 mg/cm^2 and the average of the charge-to-mass ratio of the toner was $-15 \text{ } \mu\text{C/g}$. The thickness of the PET layer was $55 \text{ } \mu\text{m}$.

In the simulation, the averages of nonelectrostatic adhesion force of toner-with-PET and toner-with-toner were set to 15 and 5 nN, according to experimental data obtained by a centrifugation method,⁸ and a Gaussian-like distribution was assumed. The adhesion force distribution of toner particles used in the simulation is shown in Figure 10. The two peaks around 15 and 5 nN were derived from two contact states of toner-on-PET and toner-on-toner, respectively.

Figure 11 shows experimental and simulated results of the applied voltage dependence of the transfer efficiency. The transfer efficiency in both experiment and simulation increased with the applied voltage up to about 900 V, and then decreased with the applied voltage. This is because the polarity of some toner particles is reversed by the discharge. Figure 12 shows the charge-to-mass ratio of the transferred

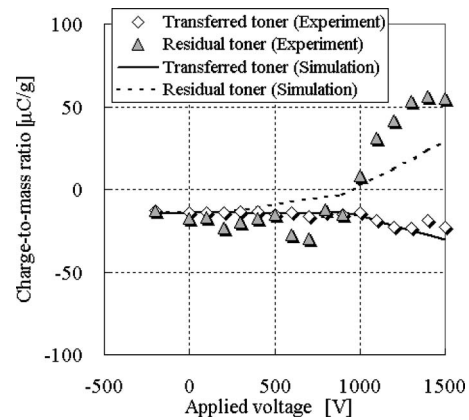


Figure 12. Applied voltage dependence of the charge-to-mass ratio of the transferred and the residual toner in the model experiment.

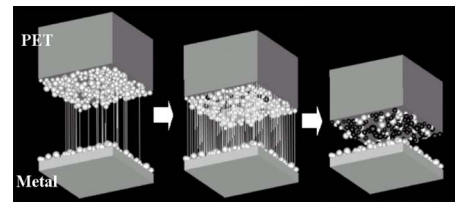


Figure 13. Snapshots of the 3D simulation. White particles are negatively charged toner, and black particles are toner particles that have been reverse charged because of the discharge. White lines in the transfer gap express the discharge.

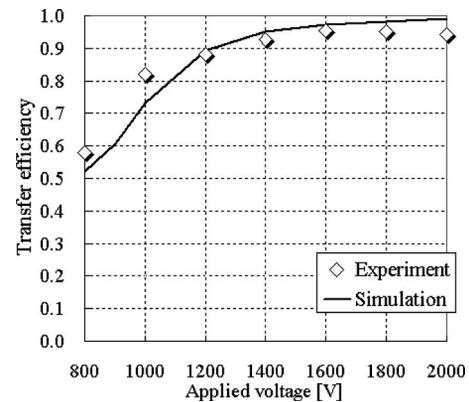


Figure 14. Relationship between the applied voltage and the transfer efficiency of the primary transfer process.

and residual toner, and shown in Figure 13 are snapshots of the simulation at 1000 V. In the case where the applied field is constant as in these experiments, the discharge is mainly caused in the approaching process, because the electric field in the separating process is weaker than that in the approaching process due to the discharge. As a result, some toner particles on the PET receive a positive charge before being transferred in the case of high applied voltage. The tendencies predicted by the simulation agree with the experiments, which supports the validity of the 3D model.

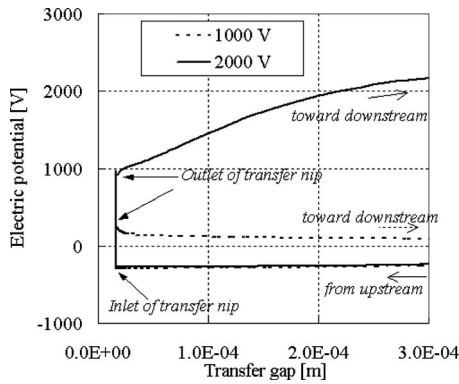


Figure 15. Relations between the electric potential of the back side of the ITB and the transfer gap in the case of the applied voltage of 1000 and 2000 V.

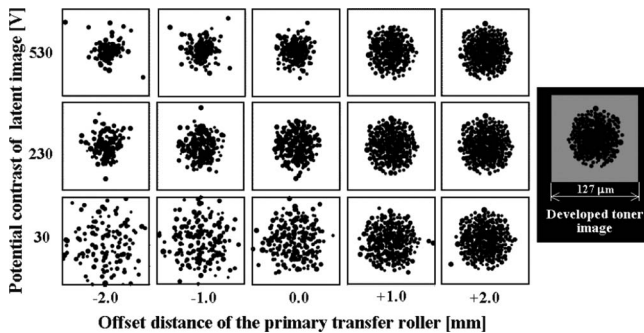


Figure 16. Transferred one-dot images simulated with various offset distance between the primary transfer roller and the OPC in the direction of the ITB motion, and with various potential contrasts between image area and nonimage area of the latent image on the OPC.

ANALYSES OF PRIMARY TRANSFER PROCESSES IN A PRINTER

Finally, analyses of a primary transfer process in a printer have been demonstrated by using the method coupling the 2D and 3D models. Figure 14 shows experimental and calculated applied voltage dependence of the transfer efficiency of a solid image that is transferred in the printer, which has been used in the 2D model validation section. The amount of developed toner is 0.65 mg/cm^2 , and the charge-to-mass ratio of the toner is $-20 \text{ } \mu\text{C/g}$. In the simulation, the averages of nonelectrostatic adhesion force of toner-with-OPC and of toner-with-toner have been set to be 15 and 5 nN, and a Gaussian-like distribution has been assumed in the same way as in the 3D validation section. In addition, shown in Figure 15 are examples of the relationship between the electric potential of the back side of the ITB and the transfer gap used in the 3D calculation. The electric potential in the prenip region is negative due to the effect of the electric charge of the toner and the OPC, and it becomes positive in the nip because of the biased primary transfer roller. Further, the potential in the postnip region increases with the transfer gap, insofar as excess positive charge is added to the ITB from the roller.

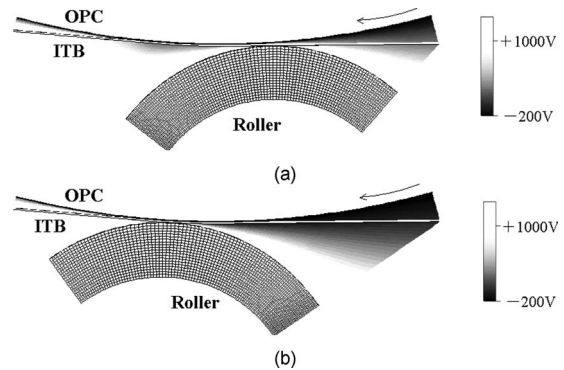


Figure 17. Electric potential distribution around transfer nips obtained by the 2D simulation. Offset distance (a) -2 mm and (b) $+2 \text{ mm}$. In these examples, the OPC initially has a uniform electric charge of -110 with $-40 \text{ } \mu\text{C/m}^2$ of a developed toner layer, and a bias voltage of 2000 V is applied to the roller. White area, except for the ITB, shows where the electric potential is higher than 1000 V .

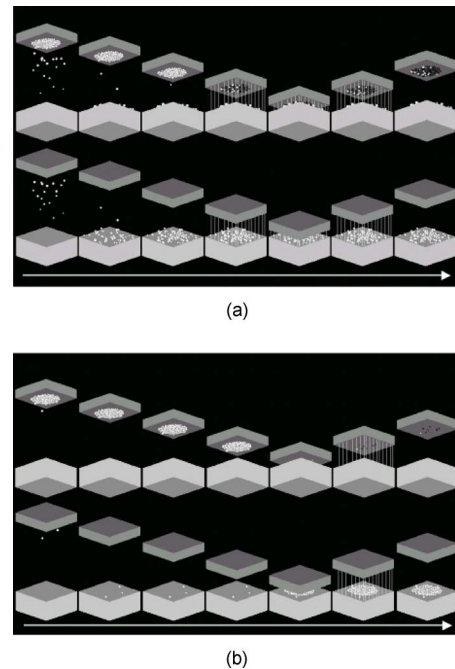


Figure 18. Snapshots of the transfer behavior on condition that the potential contrast of the latent image is 30 V . Offset distance (a) -2 mm and (b) $+2 \text{ mm}$. White particles are negatively charged toner, and black particles are toner particles that are reverse charged because of the discharge. White lines in the transfer gap express the discharge.

The applied voltage dependence of the transfer efficiency predicted by the simulation shows good agreement with that of the experiment, which suggests that transfer efficiency in printers can be predicted by the analysis models. Incidentally, the transfer efficiency curves of Fig. 14, where plateaus are observed, look different from those of Fig. 11 in the 3D model validation section. The reason is that in the printer, the low electric potential of the ITB is realized by arranging the roller downstream of the OPC, and therefore, little toner charge reversal is caused in the prenip region.

On the other hand, shown in Figure 16 are transferred one-dot images at a constant applied voltage, which are simulated with various offset distances between the primary transfer roller and the OPC in the direction of the ITB motion, and with various potential contrasts between image area and nonimage area of the latent image on the OPC. When the roller is located upstream from the OPC, the offset is expressed as a negative value.

In the results, the more upstream the location of the primary transfer roller, the greater the degradation of the image, especially in the case of the low potential contrast of the latent image, because in the case where the primary transfer roller is arranged in the upstream region, the electric potential difference between the OPC and the ITB in the prenip region becomes large, as shown in Figure 17, and toner particles on the OPC move before making contact with the ITB. Meanwhile, a weak edge electric field on the OPC is the reason toner scatterings increase in the case of the low potential contrast of the latent image. Figure 18 shows snapshots of the transfer behavior on condition that the offset distance is -2 mm and $+2$ mm, with the potential contrast of the latent image of 30 V. Although these tendencies can commonly be observed in actual printers, simulated results support the conclusion that the arrangement of primary transfer rollers in the downstream region is one useful method to obtain faithful transfer.

Results such as those shown in Fig. 16 can be obtained within hours on a commercial personal computer, and

therefore, the present simulation method is useful for design and development of printers.

CONCLUSION

A simplified simulation method coupling 2D and 3D models has been developed for analysis of primary transfer processes. The simulation method nicely reproduces transfer phenomena with a small computational load and therefore, it is useful for design and development of printers.

REFERENCES

- ¹M. C. Zaretsky, "Performance of an electrically biased transfer roller in a Kodak colorEdge CD copier", *J. Imaging Sci. Technol.* **37**, 187 (1993).
- ²N. Nakayama and H. Mukai, "Numerical simulation of electrostatic transfer process using discrete element method", *Proceedings of the Pan-Pacific Imaging Conference / Japan Hardcopy '98* (Imaging Society of Japan, Tokyo, 1998) p. 261.
- ³M. Kadonaga, "2-dimensional electrical simulation of intermediate belt transfer system", *Proceedings of the Japan Hardcopy 2001* (Imaging Society of Japan, Tokyo, 2001) p. 293 [in Japanese].
- ⁴T. Sasaki, S. Nasu, T. Nakaegawa, M. Saito, and J. Asai, "2-dimensional transfer process simulation considering toner behavior", *Proceedings of the Japan Hardcopy 2004* (Imaging Society of Japan, Tokyo, 2004) p. 287 [in Japanese].
- ⁵M. Kadonaga, T. Takahashi, and H. Iimura, "Numerical simulation of toner movement in a transfer process", *Proc. IS&T's NIP21*, (IS&T, Springfield, VA, 2005) p. 594.
- ⁶J. Frenkel, "On pre-breakdown phenomena in insulators and electronic semi-conductors", *Phys. Rev.* **54**, 647 (1938).
- ⁷R. M. Schaffert, *Electrography* (Focal Press, London, 1975) p. 522.
- ⁸H. Iimura, H. Kurosu, and T. Yamaguchi, "Effects of an external additive on toner adhesion", *J. Imaging Sci. Technol.* **44**, 457 (2000).